Arab J Geosci (2015) 8:6225–6236
DOI 10.1007/s12517-014-1615-4

ORIGINAL PAPER

# Evaluation of geotechnical parameters for urban site in southern Khamis Mushait city, southwest Saudi Arabia, using seismic refraction method

**Sattam Almadani · Abdullah Al-Amri · Mohamed Fnais · Kamal Abdelrahman · Elkhedr Ibrahim · Essam Abd El-Motaal**

Received: 17 May 2014 / Accepted: 1 September 2014 / Published online: 10 September 2014


**Abstract** This study includes the determination of the engineering physical parameters of a proposed urban expansion site at Khamis Mushait city, SW Saudi Arabia. The seismic refraction survey as a noninvasive seismic technique was used to determine the *P* wave velocity profile of the soil section in the studied site. This method provides a simplified characterization of subsurface in two-dimensional depth-velocity profiles. Seismic records obtained were processed and analyzed by SeisImager software to obtain one-dimensional *P* wave velocity (Vp) distribution. The measured *P* wave velocities were used to estimate relative density, *N* value, modulus of elasticity, uniaxial compression strength, ultimate tensile strength, ultimate bearing capacity, allowable bearing capacity, Poisson's ratio, and rock quality designation. The results indicate that the investigated site is composed mainly of two soil layers. The top layer is interpreted as loose incompetent soil sediments (alluvial sediments) to the depth of 5 m with $V_p$ ranging between 300 and 880 m/s. This layer is underlain by the second competent soil layer with thickness reaching 18 m and $V_p$ ranging between 1,097 and 2,626 m/s. The second layer is considered as the foundation layer, and its determined engineering physical parameters are vital information for the engineers in construction and urban development of this site.

**Keywords** *P* wave · Engineering parameters · Urban site · Saudi Arabia

S. Almadani (✉) · A. Al-Amri · M. Fnais · K. Abdelrahman · E. Ibrahim · E. A. El-Motaal
Geology and Geophysics Department, College of Science, King Saud University, Riyadh, KSA, Saudi Arabia
e-mail: salmadani@ksu.edu.sa

K. Abdelrahman
Seismology Department, National Research Institute of Astronomy and Geophysics, Helwan, Cairo, Egypt

E. Ibrahim
Geology Department, Faculty of Science, Mansoura University, Mansoura, Egypt

E. A. El-Motaal
Geology Department, Faculty of Science, Al-Azhar University, Cairo, Egypt

## Introduction

Seismic refraction method, as a nondestructive and low cost-effective geophysical method, is commonly used in various fields such as mining, civil, and geotechnical engineering works that interact with rock of underground structures, dams, foundations, rock slopes, tunnels, deep trenches, caverns… etc. This method is frequently employed to investigate physical and mechanical properties of rocks (D'andrea et al. 1965; Deere and Miller 1966; Youash 1970; Gardner et al. 1974; Lama and Vutukuri 1978; Inoue and Ohomi 1981; Gaviglio 1989; Yasar and Erdogan 2004; Khandelwal and Ranjith 2010). The quality of some rock materials is sometimes related to their elastic stiffness so that measurement of *P* wave velocity in such materials can often be used to indicate their quality as well as to determine elastic properties, since the seismic velocity depends on the elasticity and density of the material through which the energy is passing.

The main objective of this study is to evaluate the engineering parameters such as *N* value, rock quality, relative density, uniaxial compressive strength (UCS), ultimate tensile strength (UTS), and modulus of elasticity for the sedimentary overburden using seismic *P* wave velocity. The estimation of such parameters is important in engineering perspective especially for soil sediments in an urban expansion site that lies to the south of Khamis Mushait City, Asir region (Fig. 1). These

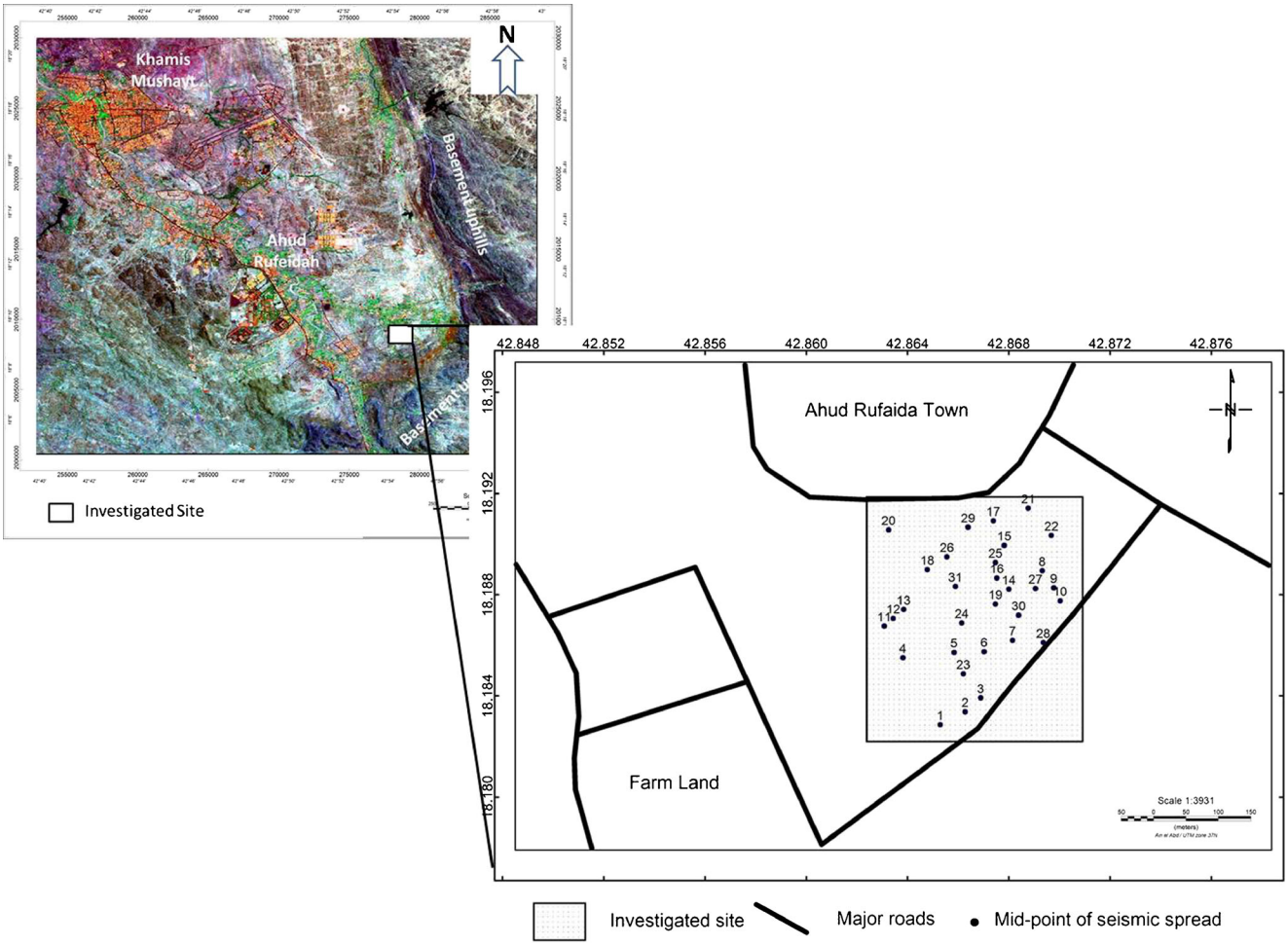


**Fig. 1** Location map of the studied site and the location of seismic refraction profiles

parameters can be taken into consideration before making important decision for civil construction in this site.

## Geological setting

Our investigated site is located south of Khamis Mushait city in Asir province in the southwest of Saudi Arabia (Fig. 1). The major portion of the studied site is underlain by Khamis Mushait Gneiss that covered with thick alluvial sedimentary soil section. Khamis Mushait Gneiss represents the main basement unit in the area that crop out along the southern, southeastern, and western sides of the investigated site (Fig. 2). These rocks are composed of banded orthogneiss, migmatite with minor amphibolite, and paragniess. This unit is invaded by numerous pegmatite dikes. The basement Gneiss rocks are covered with a thick section of alluvial soil that is composed of pebbles, gravels, sands, and clays. The alluvium soil has been transported to the investigated site by running water from the upstream and surrounding weathered Gneiss uphills through incised network of narrow and active channels.

## Data acquisition and processing

Shallow seismic refraction technique was applied at the study area to determine the dynamic properties of soil and foundation rocks. The data have been acquired along 31 shallow seismic refraction profiles (Fig. 1) using 24 channel signal enhancement seismograph "GEOMETRICS SMARTSEIS" with 5-m geophone spacing and total length of 115 m. Seismic *P* waves have been generated using a sledgehammer 10 kg at three shot points for each profile, at the 1st geophone (forward shooting), midpoint shooting (between geophones 12 and 13), and at the 24th geophone (reverse shooting). The refracted seismic waves are returned to the ground surface and recorded at the geophone points. Seismic signals were stacked at least three times for each source. Figure 3 shows a representative example of the measured raw data.

The acquired seismic row data have been processed through SeisImager/2D software Version 3.14 (Geometrics Company 2009). The collected data are first plotted and then filtered using a band-pass filter. The first arrivals are picked, and all picked first arrival travel times are used to construct travel time-distance curve for each profile. Accordingly, the

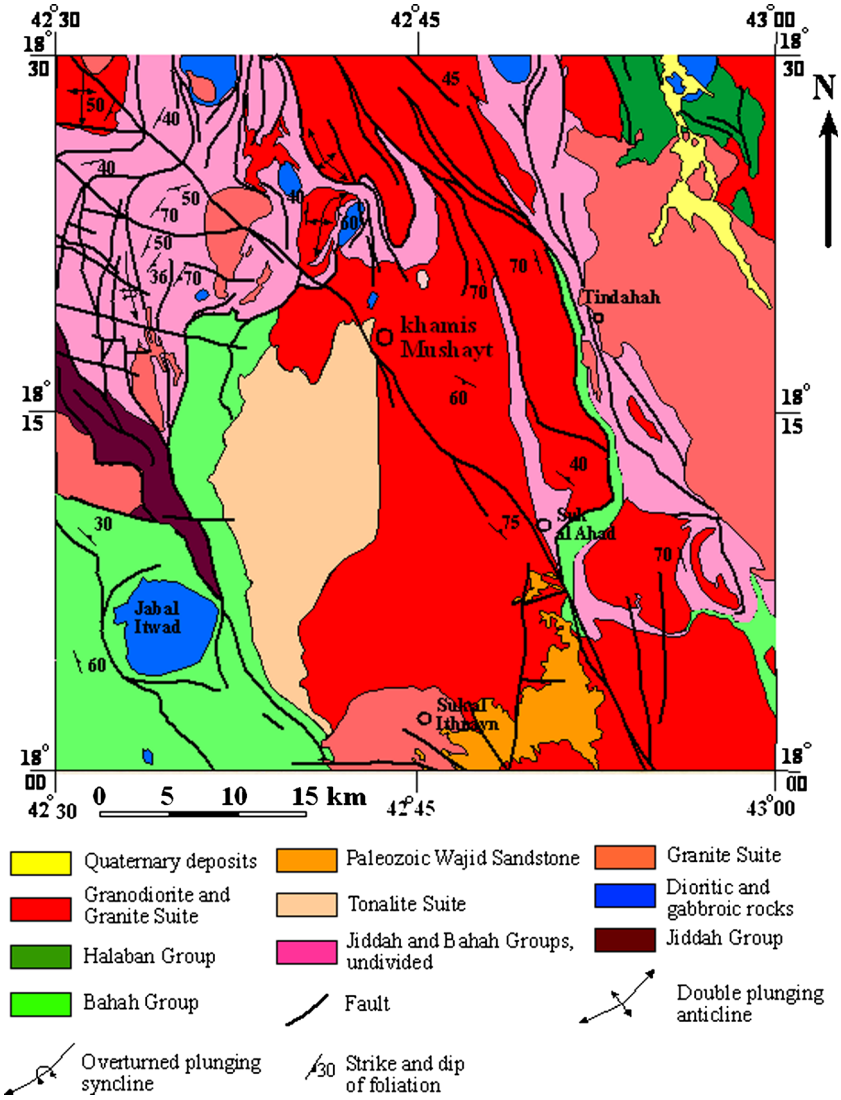


**Fig. 2** Geologic map for the studied area

subsurface layers have been assigned, and then, the corresponding velocity-depth model has been generated.

## Results and interpretation

### Seismic velocities and soil strata

Shallow seismic refraction method gives information about the subsurface structures in terms of seismic velocities and layer thicknesses (Table 1). These velocities are directly related to the quality, hardness, compaction, and water content of the medium (Altindag 2012; Khandelwal 2013). However, as qualitative classification, seismic velocities are classified into three velocity ranges that are used for identifying the subsurface rock layers in terms of the compaction and stiffness of the soil sediments and hard bedrock (Table 2). In this study, the constructed depth-velocity model clarified three subsurface layers; the surface layer exhibits a *P* wave velocity of about 300 to 880 m/s, these velocities correspond to the surface loose sediment zone with thickness that varies from 1 to 5 m. The second layer shows that *P* wave velocity ranges from 1,097 to 2,490 m/s that could be correlated to compact sediments with thickness that varies between 3 and 28 m. The third layer shows a *P* wave velocity between 2,100 and 5,277.5 m/s that could be assigned for Khamis Mushait Gneiss. The calculated thickness and velocities of the interpreted seismic layers are listed in Table 1, displayed on maps (Fig. 4) and plotted in 2D cross sections showing the distribution of the subsurface layers (Fig. 5).

### Geotechnical parameters

#### *Relative density*

The relationship between *P* wave velocity and rock density has been investigated by many researchers (e.g., Brich 1960; Kopf et al. 1985). There is a direct relation between the

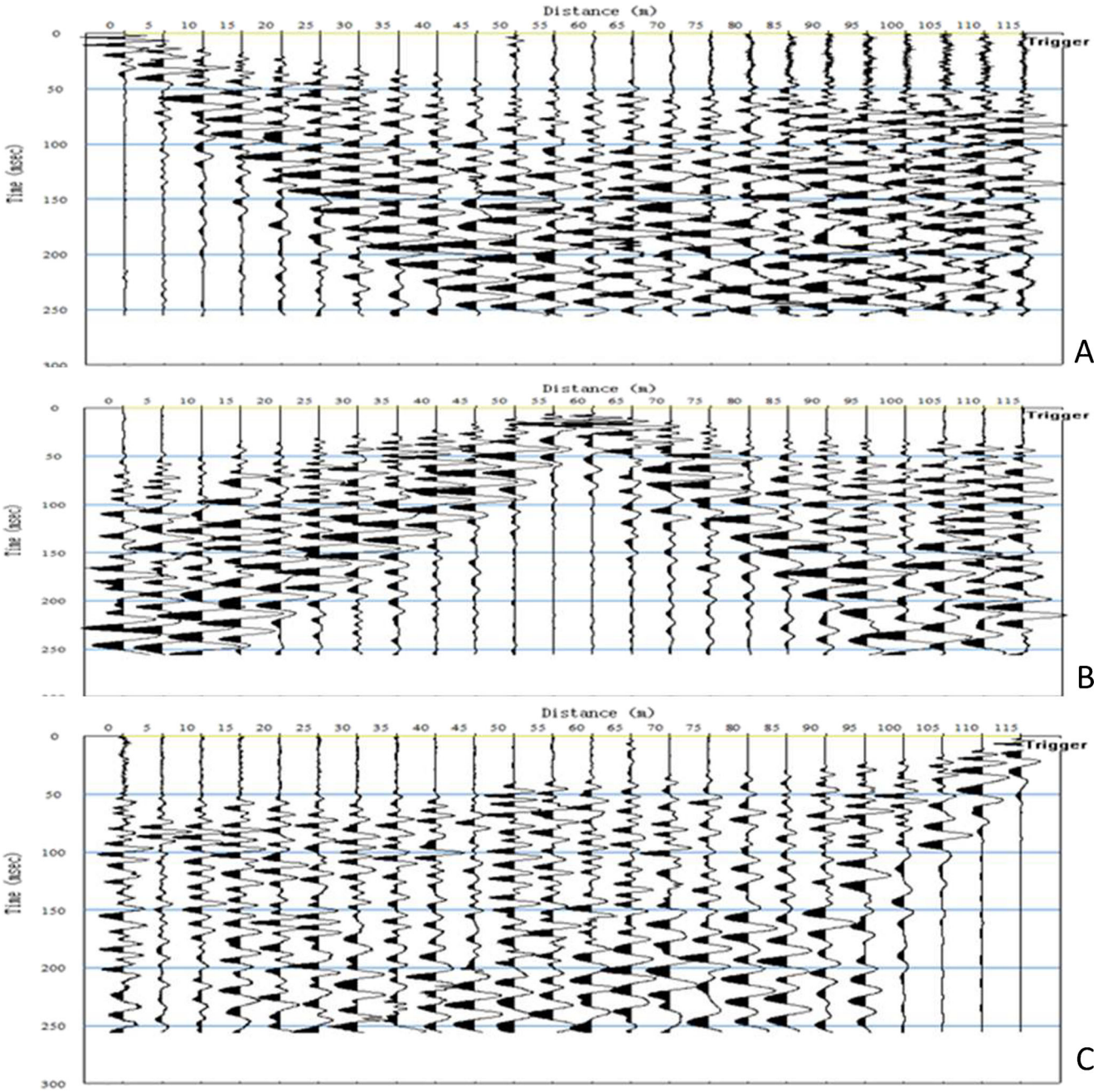


**Fig. 3** Representative example of forward (**a**), midpoint (**b**), and reverse shooting (**c**) seismogram for profile no.1

material competence, the value of the density, and the compression velocity ($V_p$). The most common relation between density (ρ) and $P$ wave velocity ($V_p$) was introduced by Gardner et al. (1974):

$$\rho = 0.31 Vp^{0.25} \quad (1)$$

Based on this empirical equation, the density of the subsurface soil section is calculated. The distribution of the density in the first layer ranges from 1.29 to 1.59 (Fig. 6a and Table 2). The relatively low values dominate the southern and northern parts of the study area, which indicates the relatively fair competent soil. The higher values are observed in the central part of the study area, reflecting a good competent soil. The density of the second layer ranges from 1.95 to 2.19 (Fig. 6b and Table 3). The relatively low values are observed in the western and eastern parts of the study area, indicating a relatively fair competent soil. In contrast, the higher values extend from the south to north in the central zone of the study area, reflecting good competent materials.

**Table 1** Interpreted seismic *P* wave velocities and thicknesses of the interpreted seismic layers

| Line no. | First layer | | Second layer | | Third layer |
|---|---|---|---|---|---|
| | Vp1 m/s | h1 (m) | Vp2 m/s | h2 (m) | Vp3 m/s |
| 1 | 300 | 2.4 | 2,093.6 | 14 | 5,189.6 |
| 2 | 300 | 3 | 1,586.7 | 9 | 5,065.3 |
| 3 | 261.8 | 3 | 1,365.8 | 18 | 5,277.5 |
| 4 | 675.4 | 4.5 | 2,432.3 | 7 | 5,003 |
| 5 | 617.2 | 3.8 | 1,801.4 | 12 | 4,831 |
| 6 | 708.3 | 2 | 2,114.3 | 28 | 5,000 |
| 7 | 433.5 | 2 | 1,360.4 | 6.5 | 4,827 |
| 8 | 482.4 | 3 | 1,306.7 | 10 | 4,531 |
| 9 | 541.8 | 2 | 1,441.1 | 9 | 4,937 |
| 10 | 880.7 | 3 | 1,547.1 | 11 | 4,720.2 |
| 11 | 732.9 | 1 | 2,241 | 5 | 4,643 |
| 12 | 659 | 4 | 2,103 | 4 | 4,001 |
| 13 | 601 | 5 | 2,490 | 5 | 3,974 |
| 14 | 555.5 | 2.2 | 2,250 | 6.9 | 5,000 |
| 15 | 521.6 | 1 | 2,249.3 | 13 | 3,986.5 |
| 16 | 539.3 | 3.4 | 2,184 | 11 | 3,652 |
| 17 | 600 | 1.8 | 1,300 | 9 | 3,600 |
| 18 | 528 | 2.1 | 2,045 | 14 | 4,673 |
| 19 | 632 | 1 | 2,142 | 8 | 3,892 |
| 20 | 500 | 3 | 1,800 | 3 | 2,100 |
| 21 | 433.4 | 3 | 1,679 | 7 | 3,730 |
| 22 | 361.2 | 4 | 1,893.7 | 19 | 3,671.8 |
| 23 | 530 | 3.5 | 1,400 | 9 | 2,130 |
| 24 | 300 | 2 | 1,097 | 8.5 | 2,542.9 |
| 25 | 300 | 3 | 1,577 | 10 | 2,439 |
| 26 | 479.7 | 2 | 2,392.2 | 18 | 4,183 |
| 27 | 586.5 | 2 | 2,156.8 | 5 | 4,216.9 |
| 28 | 603.8 | 5 | 2,489.7 | 3 | 4,986.3 |
| 29 | 563.4 | 1.6 | 1,895.9 | 11 | 4,101.6 |
| 30 | 711.3 | 2.7 | 2,292 | 5 | 4,379 |
| 31 | 573.8 | 3.2 | 2,283 | 10 | 4,739 |

*Standard penetration test (SPT)*

SPT test (or *N* value) is a dynamic test that measures the density of the soil. Several relationships have been established between *P* wave velocity and SPT. In the present study, the empirical equation of Bery and Saad (2012) has been used for *N* value estimation for the first layer based on *P* wave velocity values for soil materials as follow:

$$\mathbf{V_p} = 23.605(\mathbf{N}) - 160.43 \quad (2)$$

The estimated *N* value for the first layer (Fig. 6a and Table 2) varies from 21 to 34. The relatively low values dominate the southern and northern parts of the study area, which indicates the relatively loose soil materials. The higher values are observed in the central part of the study area, reflecting fair dense materials in this part of the study area. The value of *N* is calculated for the surface soil layer only because the *N* value of the second layer exceeds 50 (Table 3), indicating a soft rock according to Table 4.

*Rock quality designation (RQD)*

RQD forms a basic element in some of the most used rock mass classification systems: Rock Mass Rating system (RMR) and Q-system. RQD is defined in equation as

$$\boldsymbol{RQD} = \left[\frac{\boldsymbol{l}_{\boldsymbol{sum\ of\ 100}}}{\boldsymbol{l}_{\boldsymbol{tot\ core\ run}}}\right] \times \mathbf{100}\% \quad (3)$$

where $l_{\text{sum of 100}}$=sum of length of core sticks longer than 100 mm measured along the center of the core and $l_{\text{tot core run}}$= total length of core run.

In this study, *P* wave velocity that estimated from seismic survey has been used to calculate the RQD for the second layer using the equation of Bery and Saad (2012) with regression of 0.8377 (83.77 %) as follows:

$$\boldsymbol{V_p} = 21.951(\boldsymbol{RQD}) + 0.1368 \quad (4)$$

According to Table 3 and Fig. 6b, RQD values for the second layer more than 75 % indicate that this layer is composed of a rock of good quality (Table 3).

*Uniaxial compression strength (UCS)*

There are many relationships between UCS and *P* wave velocity (Mccann et al. 1990; Cheng and Hu 2003; Entwisle et al. 2005; Singh and Kripamoy 2005; Chary et al. 2006; Sharma and Singh 2008). The majority of the equations yield linear and power relationships between the UCS and *P* wave velocity. A power correlation was found between the UCS and *P* wave velocity for the entire dataset. According to Altindag (2012), the values of UCS have been calculated using the following equation:

$$\boldsymbol{UCS} = 12.743\ \boldsymbol{Vp}^{1.194} \quad (5)$$

where UCS is the uniaxial compressive strength (MPa) and *Vp* is the *P* wave velocity (km/s). The correlation coefficient of the relationship is 0.76.

The distribution of the UCS values of the first layer ranges from 3.2 to 8.3 MPa (Fig. 6a and Table 2). The relatively low values dominate the southern and northern parts of the study area, which indicates the relatively fair competent soil. The higher values are observed in the central part of the study area, reflecting a good competent soil. Figure 6b illustrates the distribution of UCS for the second layer that ranges from

**Table 2** Geotechnical parameters for the first soil layer

| Line no. | ρ2 (kg/m$^3$) | *N* | E (GPa) | UCS (MPa) | UTS (MPa) | Qult (KPa) | Qa (KPa) | σ |
|---|---|---|---|---|---|---|---|---|
| 1 | 1.29 | 19.50561 | 0.091932 | 3.026596 | 0.273509 | 585.1684 | 292.5842 | 0.21672 |
| 2 | 1.29 | 19.50561 | 0.091932 | 3.026596 | 0.273509 | 585.1684 | 292.5842 | 0.21672 |
| 3 | 1.247 | 17.88731 | 0.070853 | 2.572334 | 0.234742 | 536.6194 | 268.3097 | 0.217312 |
| 4 | 1.58 | 35.40902 | 0.433913 | 7.975677 | 0.679954 | 1062.271 | 531.1354 | 0.212141 |
| 5 | 1.545 | 32.94344 | 0.365231 | 7.162097 | 0.614557 | 988.3033 | 494.1517 | 0.212703 |
| 6 | 1.599 | 36.8028 | 0.475227 | 8.441722 | 0.717232 | 1104.084 | 552.0419 | 0.211848 |
| 7 | 1.415 | 25.16119 | 0.185852 | 4.697174 | 0.413405 | 754.8358 | 377.4179 | 0.214833 |
| 8 | 1.453 | 27.23279 | 0.227996 | 5.336543 | 0.466086 | 816.9837 | 408.4918 | 0.214214 |
| 9 | 1.496 | 29.74921 | 0.284684 | 6.130211 | 0.530958 | 892.4762 | 446.2381 | 0.213512 |
| 10 | 1.689 | 44.10633 | 0.720801 | 10.94955 | 0.915866 | 1323.19 | 661.595 | 0.210591 |
| 11 | 1.613 | 37.84495 | 0.507287 | 8.79296 | 0.745245 | 1135.348 | 567.6742 | 0.211639 |
| 12 | 1.571 | 34.71426 | 0.413988 | 7.74499 | 0.661454 | 1041.428 | 520.7138 | 0.212294 |
| 13 | 1.535 | 32.25715 | 0.34712 | 6.938216 | 0.596484 | 967.7145 | 483.8572 | 0.21287 |
| 14 | 1.505 | 30.32959 | 0.298607 | 6.315743 | 0.546048 | 909.8877 | 454.9439 | 0.213359 |
| 15 | 1.481 | 28.89345 | 0.264733 | 5.858315 | 0.508794 | 866.8036 | 433.4018 | 0.213745 |
| 16 | 1.494 | 29.6433 | 0.282177 | 6.096453 | 0.52821 | 889.2989 | 444.6494 | 0.213541 |
| 17 | 1.534 | 32.21479 | 0.346016 | 6.924434 | 0.595371 | 966.4436 | 483.2218 | 0.21288 |
| 18 | 1.486 | 29.16458 | 0.270979 | 5.944243 | 0.515805 | 874.9375 | 437.4688 | 0.21367 |
| 19 | 1.554 | 33.57043 | 0.382161 | 7.367631 | 0.631118 | 1007.113 | 503.5564 | 0.212555 |
| 20 | 1.466 | 27.97839 | 0.244166 | 5.569829 | 0.485211 | 839.3518 | 419.6759 | 0.214 |
| 21 | 1.414 | 25.15696 | 0.18577 | 4.695881 | 0.413298 | 754.7087 | 377.3544 | 0.214835 |
| 22 | 1.351 | 22.09828 | 0.131111 | 3.777657 | 0.336861 | 662.9485 | 331.4743 | 0.21582 |
| 23 | 1.487 | 29.24931 | 0.272945 | 5.971137 | 0.517999 | 877.4793 | 438.7397 | 0.213647 |
| 24 | 1.29 | 19.50561 | 0.091932 | 3.026596 | 0.273509 | 585.1684 | 292.5842 | 0.21672 |
| 25 | 1.29 | 19.50561 | 0.091932 | 3.026596 | 0.273509 | 585.1684 | 292.5842 | 0.21672 |
| 26 | 1.451 | 27.11841 | 0.225562 | 5.300899 | 0.463159 | 813.5522 | 406.7761 | 0.214247 |
| 27 | 1.526 | 31.64287 | 0.331282 | 6.738817 | 0.580359 | 949.2862 | 474.6431 | 0.213022 |
| 28 | 1.537 | 32.37577 | 0.350219 | 6.976829 | 0.599604 | 971.273 | 485.6365 | 0.212841 |
| 29 | 1.51 | 30.66427 | 0.30678 | 6.423134 | 0.55477 | 919.928 | 459.964 | 0.213271 |
| 30 | 1.6 | 36.92989 | 0.479083 | 8.484431 | 0.720642 | 1107.897 | 553.9483 | 0.211822 |
| 31 | 1.517 | 31.10485 | 0.3177 | 6.564955 | 0.566275 | 933.1455 | 466.5728 | 0.213158 |

$\rho$ relative density, *N* value standard penetration test (SPT), *E* modulus of elasticity, *UCS* uniaxial compression strength, *UTS* ultimate tensile strength, $Q_{ult}$ ultimate bearing capacity, *Qa* allowable bearing capacity, $\sigma$ Poisson's ratio, *RQD* rock quality designation

22.36 to 38.98 MPa (Table 3). The relatively low values are observed in the northeastern and southeast parts of the study area, indicating a relatively incompetent soil, while the higher values extend from the east to west in the middle part of the study area, reflecting good to fair competent materials. These higher values are intruded by a long and narrow low value strip that could be referred to narrow wadi channel that drains from the southwestern Khamis Mushait Gneiss hills (Almadani et al. 2014). This channel is characterized by its thick loose alluvial soil (Fig. 4).

*Ultimate tensile strength*

The *UTS* of a material is the limit stress at which the material actually breaks, with sudden release of the stored elastic energy. The relation between tensile strength versus *Vp* can be expressed by the following equation (Altindag 2012):

$$\boldsymbol{UTS} = 1.0562\,\boldsymbol{Vp}^{1.1222} \tag{6}$$

where *UTS* is the tensile strength (MPa) and *Vp* is the *P* wave velocity (km/s). The correlation coefficient of the relationship is 0.77.

The UTS estimated values are shown in Tables 2 and 3 and Fig. 6a, b for the first and second interpreted layers. Figure 6a indicates the UTS for the first layer and varies between 0.2 and 0.7 MPa. The relatively low values dominate the southern and northern parts of the study area, which indicates the relatively fair competent soil, while the high values are observed in the

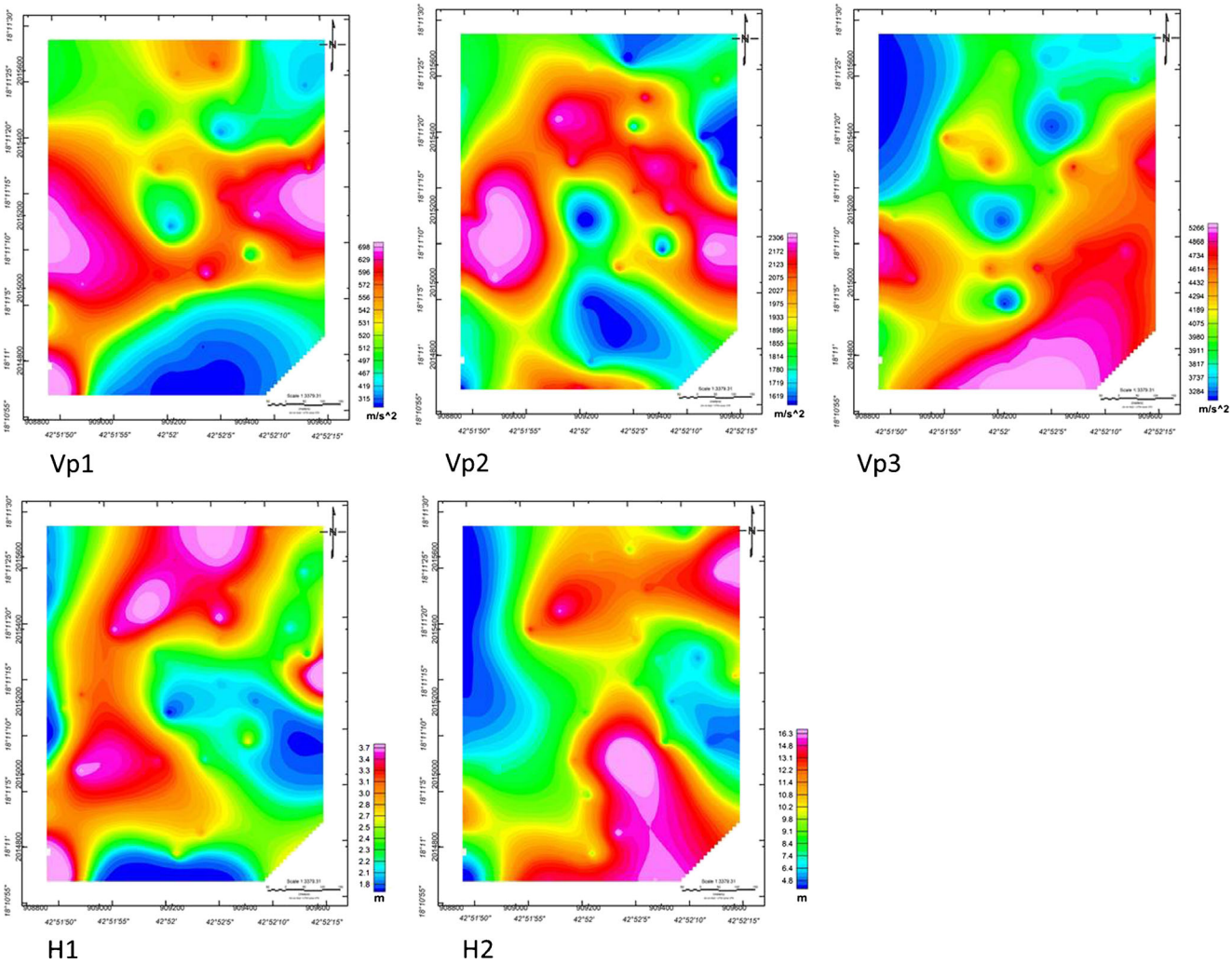


**Fig. 4** Maps show the distribution of the seismic velocities and thicknesses of the two soil layers. Vp1, Vp2, and Vp3 are the *P* wave velocities of the first, second, and third layers. H1 and H2 are the thicknesses of the first and second layers

central part of the study area, reflecting a good competent soil. Figure 6b illustrates the distribution of UTS values for the second layer where they range from 1.78 to 3.01 MPa. The relatively low values are observed in the northwestern and southwestern parts of the study area, indicating a relatively incompetent soil, while the higher values extend from the east to west in the middle part of the study area, reflecting good to fair competent soil materials. This high values are intruded by a long and narrow low values strip that could be referred to narrow wadi channel that drains from the southwestern Khamis Mushait Gneiss hills (Almadani et al. 2014). This channel is characterized by its thick loose alluvial soil (Fig. 4).

*Modulus of elasticity (**E**)*

There is a power relationship between modulus of elasticity (*E*) and *P* wave velocity (Altindag 2012):

$$\boldsymbol{E} = 0.919\boldsymbol{Vp}^{1.9122} \tag{7}$$

where *E* is the modulus of elasticity (GPa) and *Vp* is the *P* wave velocity (km/s). The correlation coefficient of the relationship is 0.79.

The estimated values of modulus of elasticity for first and second layers are presented in Tables 2 and 3 and Fig. 6a, b as well. Figure 6a indicates the *E* for the first layer and varies between 0.07 and 0.72 GPa. The relatively low values dominate the southern and northern parts of the study area, which indicates the relatively fair competent soil. While the high values are observed in the central part of the study area, reflecting a good competent soil.

Figure 6b illustrates the distribution of *E* values for the second layer which ranges from 1.09 to 7.66 GPa. The relatively low values are observed in the northwestern and southwestern parts of the study area, indicating a relatively incompetent soil. While the higher values extend from the east to west in the middle part of the study area, reflecting good to fair competent soil materials. These higher values are intruded by a long and narrow low values strip that could be referred to

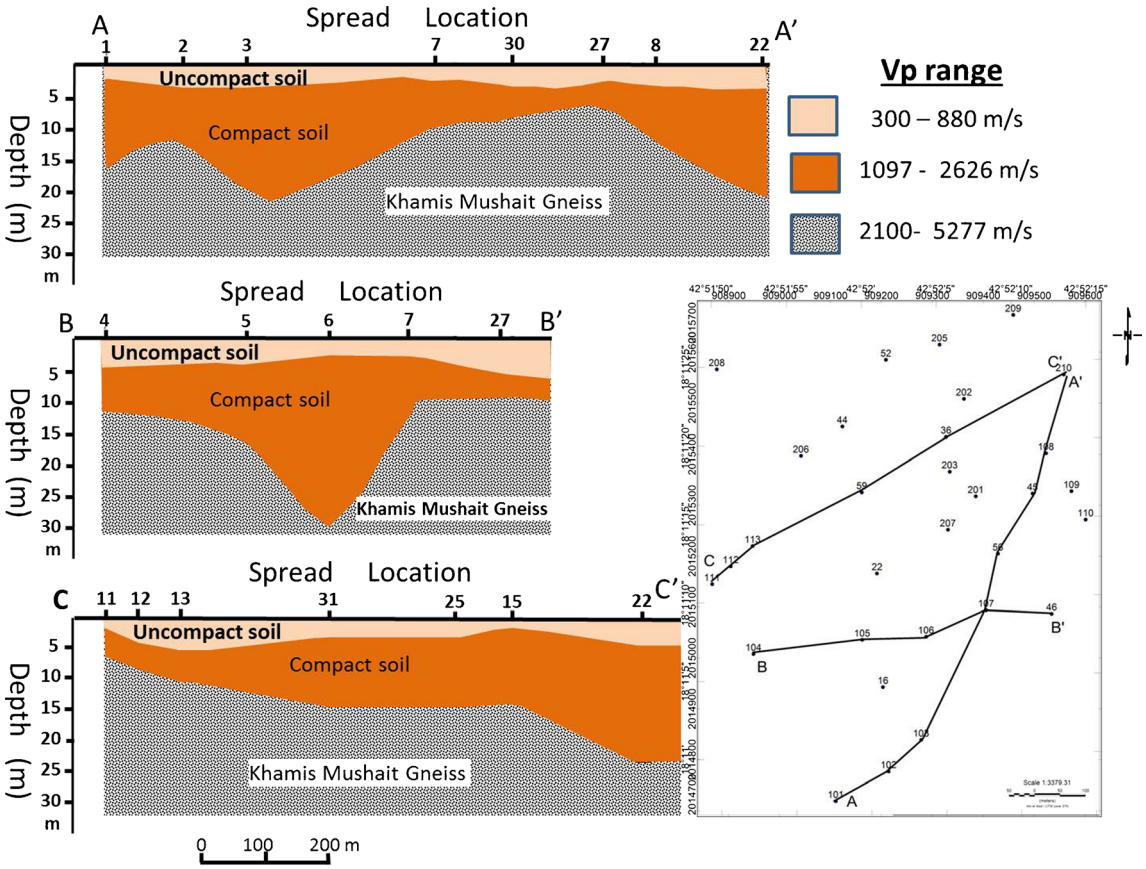


**Fig. 5** 2D depth-velocity sections along selected three profiles and the location of the selected profiles

narrow wadi channel that drains from the southwestern Khamis Mushait Gneiss hills (Almadani et al. 2014). This channel is characterized by its thick loose alluvial soil (Fig. 4).

### *Ultimate bearing capacity ($Q_{ult}$)*

The ultimate bearing capacity ($Q_{ult}$) is defined as the maximum load required for shear failure or sand liquefaction. This capacity is controlled by shear strength factor. The ultimate bearing capacity for cohessionless soils can be calculated by using the SPT from Parry's formula (Parry 1977):

$$Q_{ult} = 30N \tag{8}$$

where $N$ value is the resistance of penetration by normalized cylindrical bars under standard load.

The estimated values of $Q_{ult}$ for the first and second layers are presented in Tables 3 and 4 and Fig. 6a, b as well. Figure 6a indicates the $Q_{ult}$ for the first layer and varies between 585.16 and 1,323.19 KPa. The relatively low values dominate the southern and northern parts of the study area, which indicates the relatively fair competent soil, while the high values are observed in the central part of the study area, reflecting a good competent soil.

Figure 6b illustrates the distribution of $Q_{ult}$ values for the second layer where they range from 2,270.93 to 3,395.8 KPa. The relatively low values are observed in the northwestern and southwestern parts of the study area, indicating a relatively incompetent soil. The higher values extend from the east to west in the middle part of the study area, reflecting good to fair competent soil materials. These high values are intruded by a long and narrow low values strip that could be referred to narrow wadi channel that drains from the southwestern Khamis Mushait Gneiss hills (Almadani et al. 2014). This channel is characterized by its thick loose alluvial soil (Fig. 4).

### *Allowable bearing capacity ($Q_a$)*

The allowable bearing capacity is the maximum load to be considerable to avoid shear failure or sand liquefaction. The allowable bearing capacity can be calculated by dividing the

**Fig. 6** Maps show the distribution of the engineering physical parameters of the first soil layer (**a**) and second layer (**b**). ρ relative density, $N$ value standard penetration test (SPT), $E$ modulus of elasticity, $UCS$ uniaxial compression strength, $UTS$ ultimate tensile strength, $Q_{ult}$ ultimate bearing capacity, $Qa$ allowable bearing capacity, $\sigma$ Poisson's ratio, $RQD$ rock quality designation

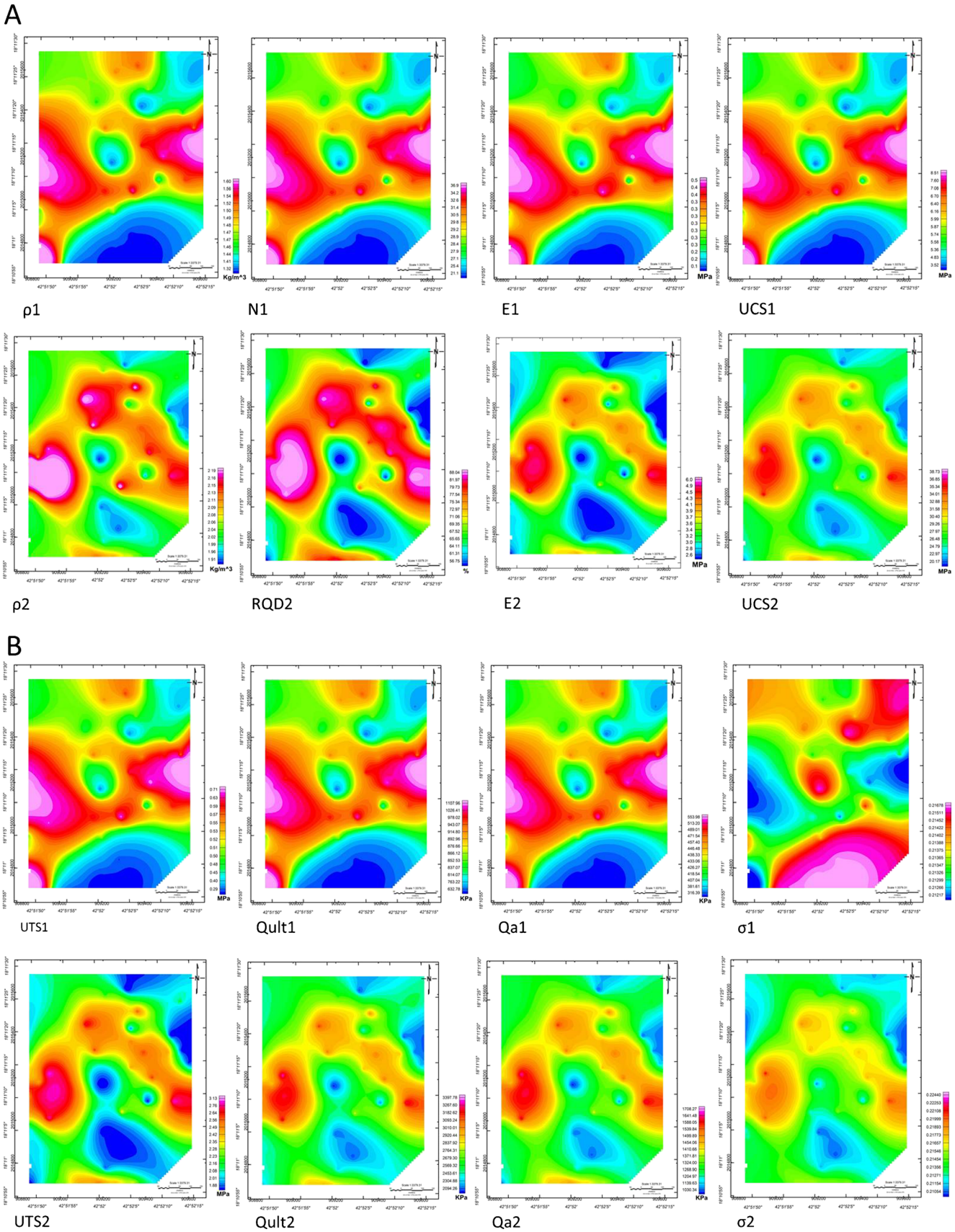
A
ρ1
N1
E1
UCS1
ρ2
RQD2
E2
UCS2
B
UTS1
Qult1
Qa1
σ1
UTS2
Qult2
Qa2
σ2

**Table 3** Geotechnical parameters for the second sedimentary layer

| Line no. | ρ2 (kg/m$^3$) | N | E (GPa) | UCS (MPa) | UTS (MPa) | Qult (KPa) | Qa (KPa) | σ | RQD |
|---|---|---|---|---|---|---|---|---|---|
| 1 | 2.096936 | 95.48951 | 3.7751 | 30.79064 | 2.42021 | 2864.685 | 1432.343 | 0.215193 | 78.3823 |
| 2 | 1.956525 | 74.01525 | 2.221783 | 22.11376 | 1.773134 | 2220.458 | 1110.229 | 0.210407 | 55.28995 |
| 3 | 1.884553 | 64.65706 | 1.668026 | 18.48945 | 1.498572 | 1939.712 | 969.856 | 0.209607 | 45.22663 |
| 4 | 2.177038 | 109.8382 | 5.02872 | 36.82783 | 2.863747 | 3295.145 | 1647.573 | 0.220683 | 93.81212 |
| 5 | 2.019595 | 83.11078 | 2.832 | 25.7318 | 2.044522 | 2493.323 | 1246.662 | 0.211932 | 65.07083 |
| 6 | 2.1021 | 96.36645 | 3.846796 | 31.15449 | 2.44708 | 2890.993 | 1445.497 | 0.215476 | 79.32531 |
| 7 | 1.882688 | 64.4283 | 1.655438 | 18.4022 | 1.491925 | 1932.849 | 966.4245 | 0.209598 | 44.98063 |
| 8 | 1.863827 | 62.15336 | 1.532735 | 17.53823 | 1.425997 | 1864.601 | 932.3004 | 0.209526 | 42.53427 |
| 9 | 1.910008 | 67.84707 | 1.848291 | 19.71299 | 1.591595 | 2035.412 | 1017.706 | 0.209792 | 48.657 |
| 10 | 1.944202 | 72.33764 | 2.11696 | 21.45639 | 1.723549 | 2170.129 | 1085.065 | 0.210206 | 53.48594 |
| 11 | 2.132908 | 101.734 | 4.299624 | 33.39637 | 2.612234 | 3052.019 | 1526.009 | 0.217357 | 85.09725 |
| 12 | 2.099286 | 95.88774 | 3.807578 | 30.95578 | 2.432408 | 2876.632 | 1438.316 | 0.215321 | 78.81052 |
| 13 | 2.189836 | 112.2826 | 5.259299 | 37.87335 | 2.940093 | 3368.477 | 1684.239 | 0.221801 | 96.4407 |
| 14 | 2.135046 | 102.1152 | 4.332703 | 33.55657 | 2.624009 | 3063.457 | 1531.728 | 0.2175 | 85.50726 |
| 15 | 2.13488 | 102.0856 | 4.330126 | 33.54411 | 2.623093 | 3062.567 | 1531.284 | 0.217489 | 85.47537 |
| 16 | 2.119214 | 99.31921 | 4.092931 | 32.38466 | 2.537789 | 2979.576 | 1489.788 | 0.216479 | 82.50056 |
| 17 | 1.861434 | 61.86952 | 1.517742 | 17.43091 | 1.417795 | 1856.086 | 928.0428 | 0.20952 | 42.22905 |
| 18 | 2.084659 | 93.43063 | 3.609302 | 29.93915 | 2.357253 | 2802.919 | 1401.459 | 0.214556 | 76.16827 |
| 19 | 2.108951 | 97.53993 | 3.943742 | 31.64245 | 2.483086 | 2926.198 | 1463.099 | 0.215865 | 80.58721 |
| 20 | 2.019202 | 83.05147 | 2.827793 | 25.70793 | 2.042739 | 2491.544 | 1245.772 | 0.21192 | 65.00705 |
| 21 | 1.984378 | 77.92544 | 2.475469 | 23.65823 | 1.889288 | 2337.763 | 1168.882 | 0.210972 | 59.49477 |
| 22 | 2.044982 | 87.02097 | 3.115946 | 27.31374 | 2.162443 | 2610.629 | 1305.315 | 0.212815 | 69.27565 |
| 23 | 1.896242 | 66.10591 | 1.748806 | 19.04358 | 1.540746 | 1983.177 | 991.5886 | 0.20968 | 46.78465 |
| 24 | 1.784076 | 53.26965 | 1.09698 | 14.23241 | 1.171834 | 1598.089 | 799.0447 | 0.209687 | 32.98118 |
| 25 | 1.953528 | 73.60432 | 2.195883 | 21.95244 | 1.760974 | 2208.13 | 1104.065 | 0.210355 | 54.84806 |
| 26 | 2.168009 | 108.1394 | 4.871381 | 36.10405 | 2.810818 | 3244.181 | 1622.091 | 0.219937 | 91.98532 |
| 27 | 2.112585 | 98.16691 | 3.996012 | 31.90367 | 2.502347 | 2945.007 | 1472.504 | 0.216078 | 81.26144 |
| 28 | 2.18977 | 112.2699 | 5.258088 | 37.8679 | 2.939696 | 3368.096 | 1684.048 | 0.221795 | 96.42703 |
| 29 | 2.045576 | 87.11417 | 3.122872 | 27.35164 | 2.165263 | 2613.425 | 1306.713 | 0.212837 | 69.37587 |
| 30 | 2.144941 | 103.8945 | 4.488672 | 34.30583 | 2.679039 | 3116.835 | 1558.418 | 0.218186 | 87.42061 |
| 31 | 2.142832 | 103.5132 | 4.455029 | 34.14505 | 2.667236 | 3105.397 | 1552.699 | 0.218037 | 87.01061 |

$\rho$ relative density, $N$ value standard penetration test (SPT), $E$ modulus of elasticity, $UCS$ uniaxial compression strength, $UTS$ ultimate tensile strength, $Q_{ult}$ ultimate bearing capacity, $Qa$ allowable bearing capacity, $\sigma$ Poisson's ratio, $RQD$ rock quality designation

ultimate bearing capacity value ($Q_{ult}$) by suitable factor of safety (Abd Elrahman 1989) as follows:

$$Q_a = \frac{Q_{ult}}{F} \tag{9}$$

**Table 4** Relationship between RQD and $N$ value (Bery and Saad 2012)

| Rock quality description | RQD (%) | $N$ value |
|---|---|---|
| Very poor | Less than 25 | 50–65 |
| Poor | 25–50 | 65–70 |
| Fair | 50–75 | 70–75 |
| Good | 75–85 | 75–85 |
| Excellent | Over 85 | Over 85 |

The safety factor ($F$) equals 2 when the soil is cohessionless material. The calculated values of $Q_a$ for first and second layers are presented in Tables 3 and 4 and Fig. 6a, b as well. Figure 6a indicates the $Q_a$ for the first layer that varies between 302.06 and 545.54 KPa. The relatively low values dominate the southern and northern parts of the study area, which indicates the relatively fair competent soil, while the high values are observed in the central part of the study area, reflecting a good competent soil.

Figure 6b illustrates the distribution of $Q_a$ values for the second layer where they range from 1,113.74 to 1,718.38 KPa. The relatively low values are observed in the western and eastern parts of the study area, indicating a relatively fair competent soil, while the higher values extend

from the south to north in the central zone of the study area, reflecting good competent soil materials.

*Poisson's ratio (σ)*

It is a fundamental parameter usually estimated in engineering studies as a ratio between the fractional transverse contraction and the fractional longitudinal extension (Bowles 1984). A suggested range for the values of Poisson's ratio is from 0.0 for very hard material to 0.5 for liquids and about (0.25) for elastic material (Sjogren 1984). In soil mechanics, the Poisson's ratio often ranges between 0.2 and 0.4 and about (0.5) for saturated soil (Hunt 1986).

The values of Poisson's ratio are calculated according to its relation with the *P* wave velocity (Khandelwal 2013) by the following equation:

$$\sigma = 8 * 10^{-9} * (V_p)^2 - 2 * 10^{-5} * (V_p) + 0.222 \qquad (10)$$

The values of Poisson's ratio for the first and second layers are illustrated in Tables 3 and 4 and Fig. 6a, b. Figure 6a shows the distribution of Poisson's ratio (σ) values for the first layer which is characterized by wide range of values of Poisson's ratio lies in the range between 0.212 and 0.217 kg/m$^3$ because of the lithological changes and the variations in degree of consolidation. This range indicates that the sediments of this layer lie between fairly to moderate competent soil.

Figure 6b illustrates the distribution of σ values for the second layer that ranges from 0.211 to 0.225 kg/m$^3$. The relatively low values are observed in the northwestern and southwestern parts of the study area, indicating a relatively incompetent soil, while the higher values extend from the east to west in the middle part of the study area, reflecting good to fair competent soil materials. These high values are intruded by a long and narrow low values strip that could be referred to narrow wadi channel that drains from the southwestern Khamis Mushait Gneiss hills (Almadani et al. 2014). This channel is characterized by its thick loose alluvial soil (Fig. 4).

## Discussions and conclusions

In this study, three seismic layers have been assigned at the site of interest from seismic refraction survey. The first and second layers represent the sedimentary overburden that covers Khamis Mushait Gneiss. This sedimentary overburden varies in thickness and velocity laterally through the area of study. The change in the thickness of this sedimentary cover could be referred to the variation in the surface topography of the Gneiss. In addition, the small wadi channels that cross the studied sites and convey water and sediments to the site from the surrounding hills play a great role in these lateral variations. The lateral change in the seismic *P* wave velocities could be related to the heterogeneity of the alluvial sediments.

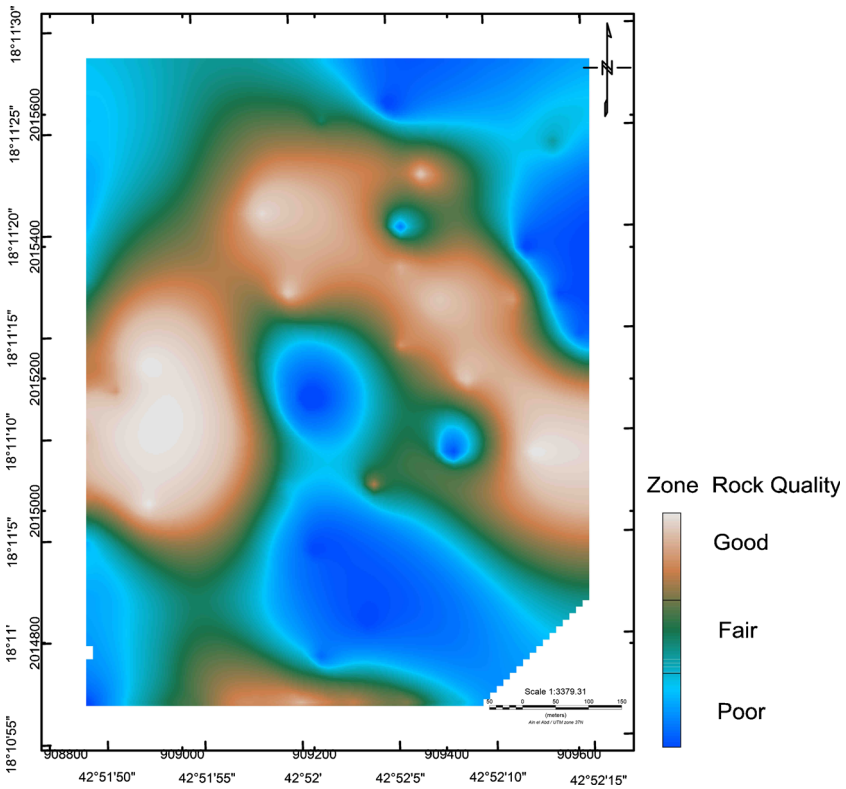


**Fig. 7** Geotechnical zonation map according to the RQD values (Table 4) for the second layer

The geotechnical parameters have been calculated for the first and second sedimentary layers based on the *P* wave velocities. According to these parameters, the second layer represents the foundation layer. This layer can be classified into three different zones according to the rock quality assessment (Fig. 7). The good competent material zone extends across the central part of the study area, representing a suitable part for engineering purposes. The north- and south-eastern parts of the site are characterized by poor rock quality and incompetent material that is considered not suitable for construction purposes. These two zones are separated and bounded by a third zone that is characterized by a fair rock quality and fair competent materials.

**Acknowledgements** The authors would like to extend their sincere appreciation to the Deanship of Scientific Research at king Saud University for funding this Research group No. RG -1435-035.

## References

Abd Elrahman MM (1989) Evaluation of the kinetic moduli of the surface materials and application to engineering geologic maps at Ma'Barrisabah area (Dhamar Province), Northern Yemen. Egypt J Geol 33:228–252

Almadani S, Ibrahim E, Abdelrahman K, Al-Bassam A, Al-Shmrani A (2014) Magnetic and seismic refraction survey for site investigation of an urban expansion site in Abha district, south west Saudi Arabia. Arab J Geosci. doi:10.1007/s12517/014/1342/x

Altindag R (2012) Correlation between P-wave velocity and some mechanical properties for sedimentary rocks. J South Afr Inst Min Metall 112:229–237

Bery AA, Saad R (2012) Correlation of seismic P-wave velocities with engineering prameters (N value and rock quality) for tropical environmental study. Int J Geosci 3:749–757

Bowles JE (1984) Physical and geotechnical properties of soils. Mc Graw-Hill International Book Company, London, 578p

Brich F (1960) The velocity of compressional waves in rocks to 10 kbars: part 1. J Geophys Res 65:1083–1102

Chary KB, Sarma LP, Lakshmi KJP, Vijayakumar NA, Lakshmi VN, Rao MV (2006) Evaluation of engineering properties of rock using ultrasonic pulse velocity and uniaxial compressive strength. Proceedings of the National seminar on Non-destructive evaluation, Hyderabad, pp 379–385

Cheng H, Hu ZY (2003) Some factors affecting the uniaxial strength of weak sandstone. Bull Eng Geol Environ 62:323–332

D'andrea DV, Fischer RL, Fogelson DE (1965) Prediction of compressive strength from other rock properties. US Bur Min Rep Invest 6702:23

Deere DU, Miller RP (1966) Engineering classification and index properties for intact rock. *Air Force Weapons Laboratory Technical Report*, AFWL-TR 65–116, Kirtland Base, New Mexico

Entwisle DC, Hobbs PRN, Jones LD, Gunn D, Raines MG (2005) The relationships between effective porosity, uniaxial compressive strength and sonic velocity of intact Borrowdale volcanic group core samples from Sellafield. Geotech Geol Eng 23:793–809

Gardner GHF, Gardner LW, Gregory AR (1974) Formation velocity and density: the diagnostic basis for stratigraphic traps. Geophysics 39: 770–780

Gaviglio P (1989) Longitudinal wave propagation in a limestone: the relationship between velocity and density. Rock Mech Rock Eng 22: 299–306

Geometrics Company (2009) SeisImager 2D software version 3.14

Hunt RE (1986) Geotechnical engineering analysis and evaluation. McGraw Hill-Ryerson, 729p

Inoue M, Ohomi M (1981) Relation between uniaxial compressive strength and elastic wave velocity of soft rock. Proceedings of the International Symposium on Weak Rock, Tokyo, pp 9–13

Khandelwal M (2013) Correlating P-wave velocity with the physico-mechanical properties of different rocks. Pure Appl Geophys 170: 507–514

Khandelwal M, Ranjith PG (2010) Correlating index properties of rocks with P-wave measurements. J Appl Geophys 71:1–5

Kopf M, Müller HJ, Gottesmann B (1985) Correlation between pyroxene content and Vp and Vs under high pressure. Kapicka, A., Kropacek, V., Pros, Z. (eds.). Physical properties of the mineral system of the Earth's Interior. *Union Czech. Math. Phys.*, Prague, pp. 168–172

Lama RD, Vutukuri VS (1978) Handbook on mechanical properties of rocks. *Trans. Tech. Publications*, Clausthal, vol. 2, Germany

Mccann DM, Culshaw MG, Northmore KJ (1990) Rock mass assessment from seismic measurements, Field Testing in Engineering Geology. Bell, Culshaw, Cripps, and Coffey (eds.). *Geological Society Publishing House, London*, vol. 6,pp. 257–266

Parry RHC (1977) Estimating bearing capacity of sand from SPT values. JGED ASCE 103:1013–1045

Sharma PK, Singh TN (2008) A correlation between *P*-wave velocity, impact strength index, slake durability index and uniaxial compressive strength. Bull Eng Geol Environ 67:17–22

Singh TN, Kripamoy S (2005) Geotechnical investigation of Amiyan landslide hazard zone in Himalayan region. Geotechnical Engineering for Disaster Mitigation and Rehabilitation, Uttaranchal

Sjogren B (1984) Shallow refraction seismics. Champman and Hall, London, 270p

Yasar E, Erdogan Y (2004) Correlating sound velocity with density, compressive strength and Young's modulus of carbonate rocks. Int J Rock Mech Min Sci 41:871–875

Youash Y (1970) Dynamic physical properties of rocks: part 2, experimental result. *Proceedings of the 2nd Congress of the International Society for Rock Mechanics*, vol. 1, Privredni Pregled, Beograd, Yugoslavia, pp. 185–195